

## **Supporting Information to:**

### **Molecular organization of cytochrome $c_2$ near the binding domain of cytochrome $bc_1$ studied by electron spin-lattice relaxation enhancement.**

Rafał Pietras, Marcin Sarewicz, Artur Osyczka

Department of Molecular Biophysics, Faculty of Biochemistry, Biophysics and Biotechnology,  
Jagiellonian University, Kraków Poland

#### **Analysis of Inversion Recovery (IR) curves**

All relaxation times were determined from analysis of Inversion Recovery curves. As this approach is often reported to be influenced by spectral diffusion we tested if this process can significantly contribute to our recovery curves. Fig. S1, A compares the results obtained from IR with those registered with the use of a saturating picket fence sequence of ten  $\pi$  pulses. We found no differences between curves obtained with the IR and the picket fence sequence therefore we concluded that under our conditions the spectral diffusion has no significant contribution to the registered recovery curves. Irrespective of the applied pulse sequence the registered recovery curves were non-single exponential.

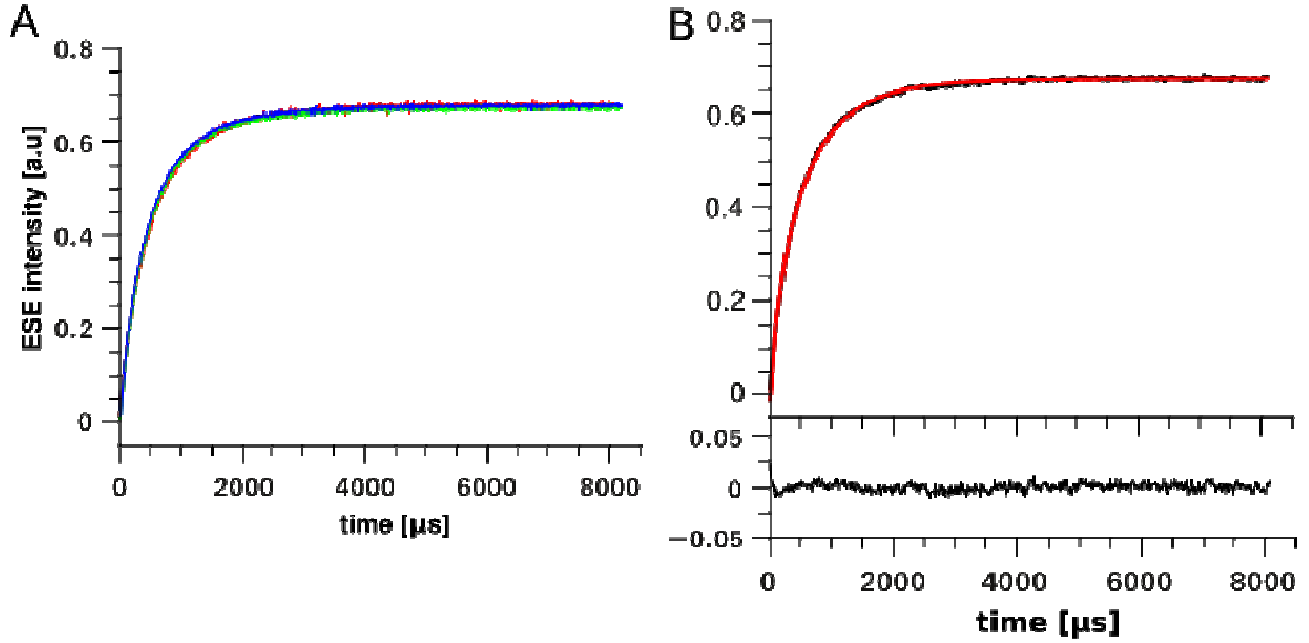


Figure S1. **Raw experimental recovery curves obtained for A101C-SL at 95K.** *A* – comparison of recovery curves obtained with the use of an IR sequence (black) with those obtained with the use of a saturating picket fence sequence of ten 40 ns  $\pi$ -pulses. Several spacing times between pulses in the picket fence sequence were tested: 100 ns (red), 1  $\mu$ s (green), 10  $\mu$ s (blue). *B* – IR curve fitted with stretched exponent. Obtained parameters were  $\tau = 491 \pm 3 \mu$ s and  $\beta = 0.807 \pm 0.004$

The recorded IR curves were normalized, multiplied by -1 and offset correction was applied. The curves were fitted with the stretched exponent function:

$$I(t) = \exp\left(-\left(t/\tau\right)^\beta\right) \quad (1)$$

This function describes a distribution of spin-lattice relaxation times<sup>1</sup>, where  $\beta \in (0,1)$  and is related to the width of the distribution, and  $\tau$  is the time constant (see Fig. S1, *B* for an example of fitting). The area under the curve can be interpreted as an average relaxation time and can be calculated as follows:

$$\tau_{avr} = \frac{\tau}{\beta} \Gamma\left(\frac{1}{\beta}\right) \quad (2)$$

where:  $\Gamma$  is the Euler gamma function.

The average spin-lattice relaxation rate is then equal to:

$$k_1 = \frac{1}{\tau_{avr}} \quad (3)$$

In all cases the extent of paramagnetic relaxation enhancement (PRE) refers to a difference in the relaxation rate for sample with PRE present ( $k_1^{PRE+}$ ) and that in which the PRE was absent ( $k_1^{PRE-}$ ):

$$k_{dip} = k_1^{PRE+} - k_1^{PRE-} \quad (4)$$

### Obtaining the binding parameters from IR measurements

To analyze the binding of cytochrome  $c_2$  to cytochrome  $bc_1$  we assumed that the process is described by a two-state model in which A101C-SL experiences different PRE in bound (to cytochrome  $bc_1$ ) and unbound forms. It follows that the measured IR curve can be represented as a sum of two components:

$$I(t) = f_b \exp\left(-\left(t/\tau_1\right)^{\beta_1}\right) + f_{ub} \exp\left(-\left(t/\tau_2\right)^{\beta_2}\right) \quad (5)$$

where:  $f_b$  is the fraction of bound A101C-SL molecules,  $\tau_1$  and  $\beta_1$  are the parameters of the stretched exponent in the bound state,  $f_{ub}$  is the fraction of unbound A101C-SL molecules,  $\tau_2$  and  $\beta_2$  are the parameters of stretched exponent of the unbound state.

Using the expression (2), one is able to calculate the area under the IR curve. This gives the representation of IR curves (Eq. 5) in terms of average spin-lattice relaxation time:

$$\tau_{avr} = f_b \tau_{avr}^b + f_{ub} \tau_{avr}^{ub} \quad (6)$$

where:  $\tau_{avr}^b$ ,  $\tau_{avr}^{ub}$  are the average relaxation times of A101C-SL in the bound and unbound states, respectively.

As  $f_b = 1 - f_{ub}$ , the equation (6) can be rewritten to describe  $\tau_{avr}$  as a function of the bound fraction of cytochrome  $c_2$ :

$$\tau_{avr} = f_b \left( \tau_{avr}^b - \tau_{avr}^{ub} \right) + \tau_{avr}^{ub} \quad (7)$$

According to Eq. (7), the average relaxation time is a linear function of bound cytochrome  $c_2$ . Thus, the

analysis of the titration of A101C-SL with cytochrome  $bc_1$  was performed with the use of the relaxation times instead of relaxation rates.

The bound fraction ( $f_b$ ) of cytochrome  $c_2$  can be expressed as a function of the total cytochrome  $bc_1$  concentration ( $P$ )<sup>2,3</sup>:

$$f_b(P) = \frac{1}{2L_0} \left( K_d + L_0 + n_a P - \left( (K_d + L_0 + n_a P)^2 - 4n_a P L_0 \right)^{\frac{1}{2}} \right) \quad (8)$$

where:  $L_0$  is the total cytochrome  $c_2$  concentration,  $K_d$  is the dissociation constant,  $n_a$  is the number of binding sites. Fitting of Eq. (7) and Eq. (8) to our data, with  $n_a$  treated as a parameter, failed to reproduce the experimental binding curves in the case of low ionic strength conditions (Fig. S2). Thus we proposed a slight modification of Eq. (8) by the replacing  $n_a$  parameter with the following function:

$$n_a = \alpha \exp(-P/L_0) + n \quad (9)$$

In the limit of  $L_0 \gg P$  (i.e. for initial points of titration) the  $n_a$  reaches the value of  $\alpha + n$ . This should be considered as a process in which many cytochrome  $c_2$  molecules are gathered near the binding domains. As the concentration of  $P$  grows, the  $n_a$  value gradually decreases reaching  $n$  under conditions where  $P \gg L_0$ . This reflects the process of dispersion of cytochrome  $c_2$  molecules to occupy the larger population of available binding sites. The comparison of the fitting of Eq. 8 before and after the modification is shown in figure S2.

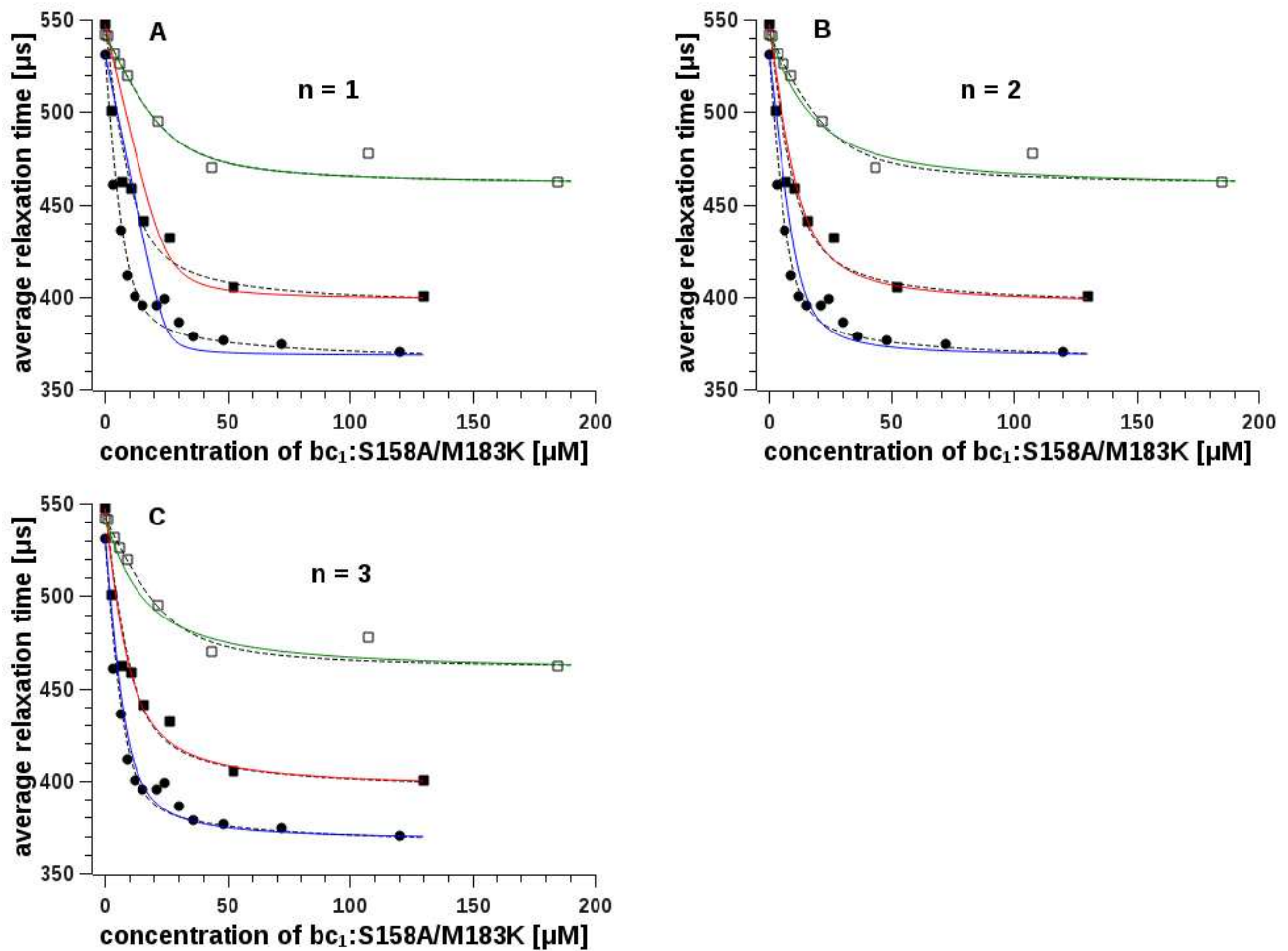


Figure S2. Comparison of models describing the cytochrome *c*<sub>2</sub> binding isotherms.

A) Results of fitting the data with model assuming  $n = 1$ . The  $K_d$  values are: 0.11, 0.6 and 5.1  $\mu\text{M}$  for 0, 10 and 25 mM NaCl respectively. B) The same as in A but using model assuming  $n = 2$ . The  $K_d$  values are: 2.7, 3.2 and 20  $\mu\text{M}$  for 0, 10 and 25 mM NaCl respectively. C) The same as in A but using model assuming  $n = 3$ . The  $K_d$  values are: 6, 12, 32  $\mu\text{M}$  for 0, 10 and 25 mM NaCl respectively. The dotted lines shows fits based on the model which assumes that number of cytochrome *c*<sub>2</sub> molecules localized near the binding domain of cytochrome *bc*<sub>1</sub> changes with the ionic strength and the cytochrome *bc*<sub>1</sub> : cytochrome *c*<sub>2</sub> molar ratio. (see Eq. 1 and Eq. 2 in the main text).

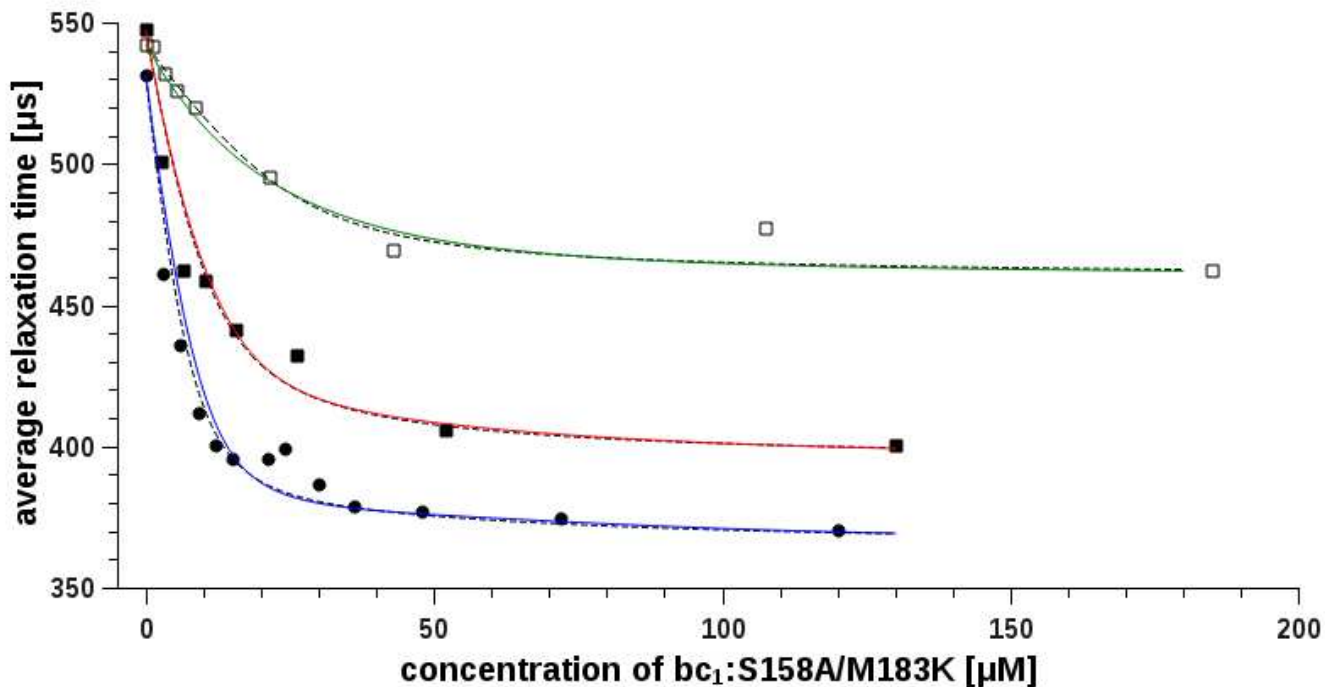


Figure S3. **Correlation between binding stoichiometry and dissociation constant ( $K_d$ )**. The data points are marked as in Fig. S2. The curves were fitted assuming two models: first with  $n = 1$  (one molecule of cytochrome  $c_2$  binds to cytochrome  $bc_1$  monomer) (black dashed lines) and the second with  $n = 0.5$  (one molecule of cytochrome  $c_2$  binds to cytochrome  $bc_1$  dimer) (colored lines). Changes in the binding stoichiometry at the same time are compensated by changes in  $K_d$  (Table S1). In both cases the fitted curves are virtually indistinguishable.

NaCl [mM]	$n = 1$		$n = 0.5$	
	$K_d$ [ $\mu$ M]	$\alpha$	$K_d$ [ $\mu$ M]	$\alpha$
0	2.7	2.1	1.1	2.1
10	3.9	1.2	1.2	1.5
25	5.1	0	1.7	0.7

Table S1. **Comparison of binding parameters** obtained from fitting the titration data with the assumption that binding stoichiometry is one cytochrome  $c_2$  per cytochrome  $bc_1$  monomer ( $n = 1$ ) and one cytochrome  $c_2$  per cytochrome  $bc_1$  dimer ( $n = 0.5$ ). For each titration experiment one can obtain two different sets of parameters that reproduce the data equally well.

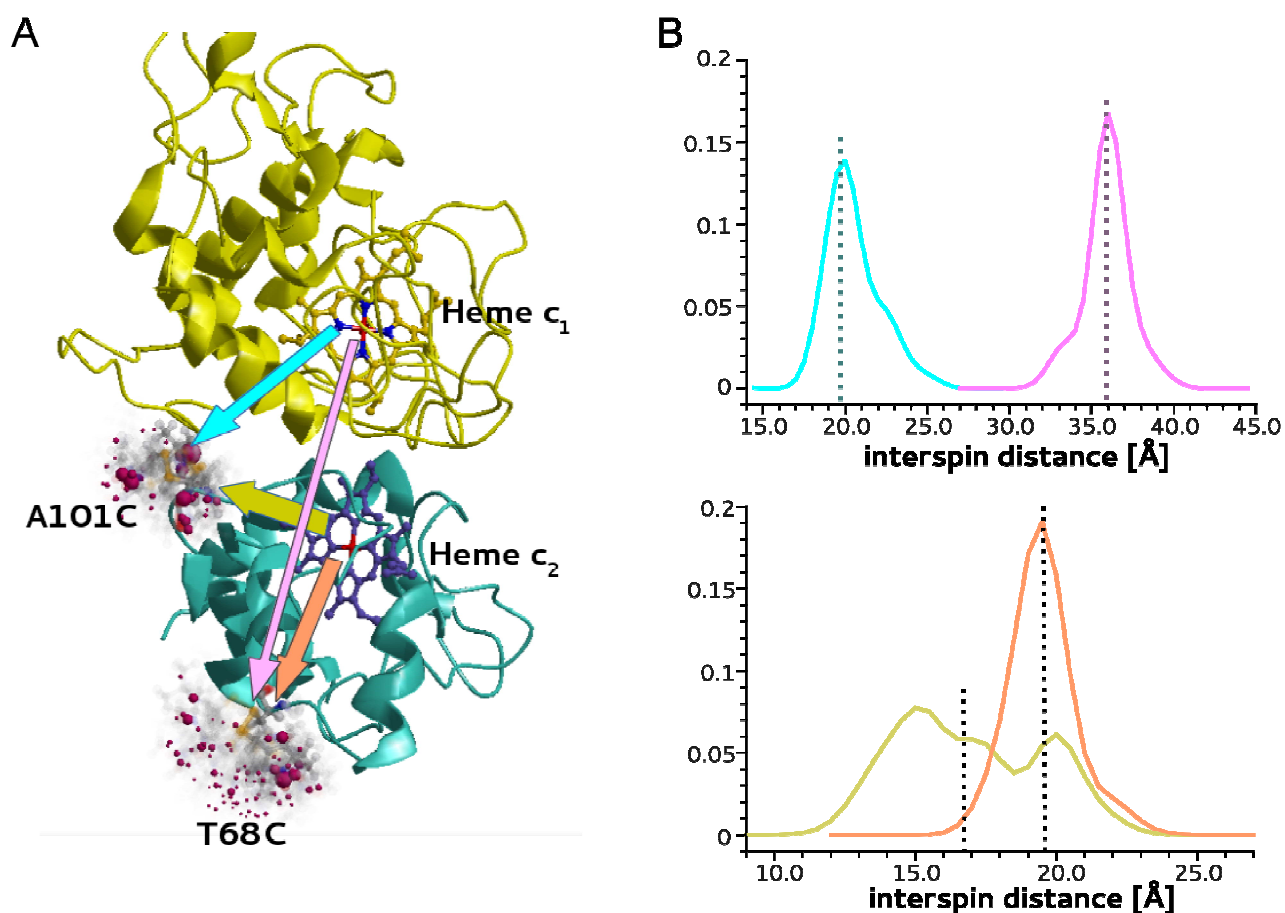


Figure S4. **Visualization of SL rotamers** on the model structure of cytochrome  $c_2$  (cyan) bound to cytochrome  $c_1$  (yellow) subunit of cytochrome  $bc_1$ . The structures of rotamers at each labeling site were obtained in MMM software with the use of MTSL rotamer library (A). Violet spheres indicate the position of NO group and their size is proportional to population. The arrows indicate four possible instances of PRE that can be observed in this system separately. The thickness of the arrows represents the strength of PRE. Distance distribution between NO groups and the iron atom of a given heme was calculated from obtained rotamer structures (B). The colors on the plots are consistent with the colors of the arrows.



## Construction of dipolar ruler

The dipolar ruler curve was constructed on the basis of Bloembergen theory<sup>4</sup>. The original formula describes the dipolar relaxation rate of a slowly relaxing center caused by a fast relaxing center. However, the exact calculation of  $k_{\text{dip}}$  can be made for a rigid system in which a distance between centers and angles between the principal g-tensor axes of interacting spins are fixed<sup>5-9</sup>. It is also needed to know the spectra, spin-spin and spin-lattice relaxation times for each interacting center. These conditions are not met in our system containing SL attached to cytochrome  $c_2$  and heme  $c_1$  in cytochrome  $bc_1$ . We were unable to determine the relaxation rate of the heme  $c_1$  iron, because its CW EPR spectrum is barely measurable, as all its transitions are overlapped by much stronger signals coming from other metal centers of cytochrome  $bc_1$ , mainly heme  $b_H$ , and the Rieske iron-sulfur cluster. In our analysis we followed the simplifications of the Bloembergen equation described in<sup>10</sup>, reaching the point where  $k_{\text{dip}}$  is approximated with a simple function:

$$k_{\text{dip}}(r) = a*r^{-6} \quad (10)$$

where:  $r$  is a distance and  $a$  is a scaling factor. The  $a$  value, that includes all non-distance-related factors of the Bloembergen equation, was determined from fitting the Eq. (10) to the points for which distances were known and  $k_{\text{dip}}$  were measured. Such an approach, similar to that previously applied<sup>11</sup>, is valid only when we assume that paramagnetic properties of heme  $c_2$  and heme  $c_1$  are comparable. Additionally we assume that for all samples the effect of changes in the relative orientation between g-tensors of SL and hemes has a negligible impact on  $k_{\text{dip}}$ <sup>12</sup> in comparison to the effect of changes in the distance.

## References

- (1) Lindsey, C. P. C.; Patterson, G. D. Detailed Comparison of the Williams–Watts and Cole–Davidson Functions. *J. Chem. Phys.* **1980**, *73*, 3348–3357.

- (2) Wang, Z. X.; Kumar, N. R.; Srivastava, D. K. A Novel Spectroscopic Titration Method for Determining the Dissociation Constant and Stoichiometry of Protein-Ligand Complex. *Anal Biochem* **1992**, *206*, 376–381.
- (3) Sarewicz, M.; Szytuła, S.; Dutka, M.; Osyczka, A.; Froncisz, W. Estimation of Binding Parameters for the Protein-Protein Interaction Using a Site-Directed Spin Labeling and EPR Spectroscopy. *Eur. Biophys. J.* **2008**, *37*, 483–493.
- (4) Kulikov, A.; Likhtenstein, G. The Use of Spin Relaxation Phenomena in the Investigation of the Structure of Model and Biological Systems by the Method of Spin Labels. *Adv. Mol. Relax. Interact. Process.* **1977**, *10*, 47–79.
- (5) Hirsh, D. D. J.; Beck, W. W. F.; Innes, J. J. B.; Brudvig, G. W. Using Saturation-Recovery EPR to Measure Distances in Proteins: Applications to Photosystem II. *Biochemistry* **1992**, *31*, 532–541.
- (6) Budker, V.; Du, J.; Seiter, M.; Eaton, G. Electron-Electron Spin-Spin Interaction in Spin-Labeled Low-Spin Methemoglobin. *Biophys. J.* **1995**, *68*, 2531–2542.
- (7) Rakowsky, M. H.; Zecevic, a; Eaton, G. R.; Eaton, S. S. Determination of High-Spin iron(III)-Nitroxyl Distances in Spin-Labeled Porphyrins by Time-Domain EPR. *J. Magn. Reson.* **1998**, *131*, 97–110.
- (8) Ulyanov, D.; Bowler, B.; Eaton, G. Electron-Electron Distances in Spin-Labeled Low-Spin Metmyoglobin Variants by Relaxation Enhancement. *Biophys. J.* **2008**, *95*, 5306–5316.
- (9) Hung, S.; Grant, C. V; Peloquin, J. M.; Waldeck, A. R.; Britt, R. D.; Chan, S. I. Electron Spin-Lattice Relaxation Measurement of the 3Fe-4S (S-3) Cluster in Succinate:Ubiquinone Reductase from *Paracoccus Denitrificans*. A Detailed Analysis Based on a Dipole-Dipole Interaction Model. *J. Phys. Chem. A* **2000**, *104*, 4402–4412.
- (10) Hirsh, D. J.; Brudvig, G. W. Measuring Distances in Proteins by Saturation-Recovery EPR. *Nat. Protoc.* **2007**, *2*, 1770–1781.
- (11) Ohnishi, T.; Schägger, H.; Meinhardt, S. W.; LoBrutto, R.; Link, T. A.; von Jagow, G. Spatial Organization of Redox Active Centers in the Bovine Heart Ubiquinol-Cytochrome c Oxidoreductase. *J. Biol. Chem.* **1989**, *264*, 735–744.
- (12) Oganessian, V. S.; White, G. F.; Field, S.; Marritt, S.; Gennis, R. B.; Yap, L. L.; Thomson, A. J. Nitroxide Spin Labels as EPR Reporters of the Relaxation and Magnetic Properties of the Heme-Copper Site in Cytochrome bo<sub>3</sub>, *E. Coli*. *J. Biol. Inorg. Chem.* **2010**, *15*, 1255–1264.